Supplementary information

Conformational switch of angiotensin II type 1 receptor underlying mechanical stress-induced activation

Noritaka Yasuda, *Shin-ichiro Miura*, *Hiroshi Akazawa*, *Toshimasa Tanaka*, *Yingjie Qin*, *Yoshihiro Kiya*, *Satoshi Imaizumi*, *Masahiro Fujino*, *Kaoru Ito*, *Yunzeng Zou*, *Shigetomo Fukuhara*, *Satoshi Kunimoto*, *Koichi Fukuzaki*, *Toshiaki Sato*, *Junbo Ge*, *Naoki Mochizuki*, *Haruaki Nakaya*, *Keijiro Saku*, *Issei Komuro*

Supplementary Methods

Materials. ^{125}I-[Sar^1, Ile^8] AngII was purchased from Amersham Biosciences. The highly reactive, sulfhydryl-specific alkylating reagent CH_3SO_2-$SCH_2CH_2NH_3^+$ (methanethiosulfonyl ethyl-ammonium [$MTSEA^+$], adduct size about 4.726 Å) was purchased from Toronto Research Chemicals. AngII and cytochalasin D were from Sigma-Aldrich, and GsMtx-4 was from Peptide Institute, Inc.

Cell cultures and transfections. HEK293 and COS7 cells were plated at a field density of $5x10^3$ cells/cm^2, and cultured in Dulbecco's modified Eagle's medium with 10% fetal bovine serum. At 24 h after seeding, all cultures were transferred to serum-free conditions 48 h before stimulation. Passive stretch of cultured cells was conducted, as described previously (Komuro et al., 1990; Zou et al., 2004). Cells were plated on collagen-coated silicone rubber dishes (STREX Mechanical Cell Strain Instruments), and silicone dishes were passively stretched by attaching both ends of the dishes firmly to a fixed frame to give a longitudinal stretch by 20% of the original length. Cells were kept stretched or left unstretched (supplementary Fig S6 online). Since the basal ERKs activities in COS7 cells are relatively higher than those in HEK293 cells, we used HEK293 cells for phosphorylation assays of ERKs in this study. WT and mutant AT_1 receptors were transfected by FuGENE 6 reagent (Roche Diagnostics) according to the manufacturer's instructions. Stable transformants were selected, as described previously (Zou et al., 2004).

Mutagenesis and expression of the AT_1 receptor and membrane preparation. The synthetic rat AT_1 receptor gene, cloned in the shuttle expression vector pMT-2, was

used for expression and mutagenesis (supplementary Tables S1 and S2), as described previously (Miura et al., 1999). Plasma membranes of transfected cells were prepared by the nitrogen Parr bomb disruption method or the freeze/thaw method in the presence of protease inhibitors.

Competition binding studies. The *K*d and *B*max values of receptor binding were determined by ^{125}I-[Sar^{1}, Ile^{8}] AngII-binding experiments under equilibrium conditions, as described previously (Miura et al., 1999). Membranes expressing the WT or mutant AT1 receptors were incubated with 100 pM ^{125}I-[Sar^{1}, Ile^{8}] AngII for 1 hr at 22℃ in a volume of 125 μl. Binding reaction was terminated by filtering the incubation mixture through Whatman GF/C glass filters, and the residues were extensively washed further with binding buffer. The bound ligand fraction was determined from the counts per minute (cpm) remaining on the membrane. Binding kinetics values were determined, as previously described (Miura et al., 1999).

Substituted cysteine accessibility mapping (SCAM). The SCAM study has been used to probe relative conformational changes of constitutively active AT_1 receptor (Boucard et al., 2003; Miura and Karnik, 2002; Miura et al., 2003) and other G protein-coupled receptors (GPCRs) (Chen et al., 2002; Jongejan et al., 2005; Lemaire et al., 2004) by validating the presence of Cys residues within the ligand pocket. We employed a highly reactive, sulfhydryl-specific reaction with methanethiosulfonyl ethyl-ammonium ($MTSEA^{+}$), which reacts a billion times faster with water-exposed and ionized Cys than lipid-exposed and un-ionized Cys. Upon this reaction, a positively charged sulfonylmethylammonium group is added onto water-exposed Cys via a mixed

disulfide bond. The chemical modification of Cys in the water-accessible ligand pocket results in interference with the ^{125}I-[Sar^1, Ile^8] AngII binding either through steric hindrance or electrostatic repulsion (Miura and Karnik, 2002; Miura et al., 2003). Transfected cells were pretreated with 10^{-7} M candesartan or candesartan-7H and stretched for 0 or 8 min in 5% CO_2 at 37°C. The cells were harvested with PBS at 4°C and cell membranes were prepared by the freeze/thaw method in the presence of protease inhibitors. The membranes were washed twice with 20 mM HEPES assay buffer (pH 7.4) at 4°C for washing out candesartan or candesartan-7H and subjected to a SCAM study. SCAM was performed, as previously described (Miura and Karnik, 2002; Miura et al., 2005; Miura et al., 2003). Briefly, aliquots of cell membranes (20 μl) were incubated with or without MTS reagent at 2 mM at 22^{o}C for 2 min in assay buffer. The reaction mix was then diluted 100-fold with cold buffer to stop the reaction and centrifuged for 10 min at 16,000 x *g* at 4^{o}C, and resuspended in 160 μl. A 75 μl aliquot was used for ^{125}I-[Sar^1, Ile^8] AngII binding analysis. The percent inhibition of ^{125}I-[Sar^1, Ile^8] AngII binding was calculated using the formula, 1-[(specific binding after MTS-reagent)/(specific binding without reagent)] x 100%. The values represent the mean ± S.D. of 4-10 independent determinations.

Western blotting. Total proteins (50 μg) were fractionated by SDS−PAGE and transferred to Hybond membranes (Amersham Biosciences). The blotted membranes were incubated with polyclonal antibody against phosphorylated ERKs (Cell Signaling), ERKs (Zymed Laboratories), phosphorylated p130Cas (Tyr165) (Cell Signaling), and p130Cas (Upstate). Horseradish peroxidase-conjugated anti-rabbit IgG antibody was

used as the secondary antibody, and signals were detected with the ECL detection kit (GE Healthcare).

Molecular modeling of the AT_1 receptor. Amino acid sequence alignment between human AT_1 receptor and bovine rhodopsin was performed using the CLUSTAL W program (Thompson et al., 1994). Since bovine rhodopsin was used as a template, "AT_1 receptor model without stretch" has almost the same backbone conformations for transmembrane helices as bovine rhodopsin crystal structure (PDB code: 1F88 (Palczewski et al., 2000)). Conformations of extracellular loops were constructed by using the Search/Generate-Loops function of Insight II while considering the following two requirements. First, the distance between the sulfur atoms of Cys^{18} and Cys^{274} must be shorter than 5 Å for presumable disulfide bridge (Ohyama et al., 1995). Second, putative N-glycosylation positions, Asn^4, Asn^{176}, and Asn^{188}, must be exposed on the surface (Lanctot et al., 1999). After a disulfide bond was formed between Cys^{18} and Cys^{274}, the whole structure was subjected to energy minimization using the MMFF94x force field in the program MOE (ver. 2005.06, Chemical Computing Group) with a harmonic force constraint against the initial atomic positions to prevent the large movement of TM helices. "AT_1 receptor model with stretch" was constructed from the model structure of "AT_1 receptor model without stretch" by inclining the extracellular end of TM7 toward TM3 around 5 degrees and by rotating TM7 a few degrees counterclockwise on Biopolymer Module of the Insight II Program (Accelyrs). "AT_1 receptor model with stretch in the presence of candesartan" was constructed by rotating TM6 and TM7 90 degrees clockwise. Candesartan was then docked into the

model using the GOLD program (ver. 2.0, Cambridge Crystallographic Data Centre), followed by energy minimization using the MMFF94x force field. The docking model fulfils both conditions in which the tetrazole group of candesartan binds to Lys^{199} (Noda et al., 1995; Takezako et al., 2004) and in which the carboxyl group of candesartan stably forms two hydrogen bonds with the side chains of Gln^{257} and Thr^{287}.

Immunocytochemistry. HEK293 cells stably expressing HA-tagged AT_1 receptor were fixed in phosphate-buffered saline (PBS) containing 4% paraformaldehyde for 30 min at 4°C, washed with PBS. The cells were stained with rat monoclonal anti-HA antibody (3F10) (Roche Diagnostics), and were visualized with FITC-conjugated goat anti-rat IgG (Chemicon). Images were acquired with a confocal microscope (Fluo View FV1000; Olympus). To visualize actin skeleton, HEK293 cells expressing AT_1 receptor, exposed to vehicle or 40 μM cytochalasin D for 10 min, were fixed in PBS containing 4% paraformaldehyde for 30 min at 4°C, washed with PBS. The cells were visualized with rhodamine-conjugated phalloidin (Molecular Probes). Images were acquired with a laser-scanning microscope (Eclipse E600; Nikon) using the Radiance 2000 confocal scanning system (Bio-Rad).

Luciferase assays. HEK293 cells were transfected with the reporter plasmid with or without the expression vector for AT_1-WT or AT_1-N111G receptor. pRL-SV40 (Promega) was co-transfected as an internal control. Luciferase activities were measured 24 h after transfection with using the Dual-luciferase reporter assay system (Promega). Experiments were repeated at least three times in triplicate, and representative data are shown. The luciferase reporter containing the *c-fos* promoter

was a generous gift from Dr. M. Tsuda (Toyama Medical and Pharmaceutical University, Japan).

Statistical analysis. The results are expressed as the mean ± S.D. of four or more independent determinations. Significant differences in measured values were evaluated with an analysis of variance using Fisher's *t*-test and an unpaired Student's *t*-test. Values of $P<0.05$ were considered statistically significant.

References

Bode, F., Sachs, F. and Franz, M.R. (2001) Tarantula peptide inhibits atrial fibrillation. *Nature*, 409, 35-36.

Boucard, A.A., Roy, M., Beaulieu, M.E., Lavigne, P., Escher, E., Guillemette, G. and Leduc, R. (2003) Constitutive activation of the angiotensin II type 1 receptor alters the spatial proximity of transmembrane 7 to the ligand-binding pocket. *J Biol Chem*, 278, 36628-36636.

Chen, S., Lin, F., Xu, M. and Graham, R.M. (2002) Phe(303) in TMVI of the alpha(1B)-adrenergic receptor is a key residue coupling TM helical movements to G-protein activation. *Biochemistry*, 41, 588-596.

Jongejan, A., Bruysters, M., Ballesteros, J.A., Haaksma, E., Bakker, R.A., Pardo, L. and Leurs, R. (2005) Linking agonist binding to histamine H1 receptor activation. *Nat Chem Biol*, 1, 98-103.

Komuro, I., Kaida, T., Shibazaki, Y., Kurabayashi, M., Katoh, Y., Hoh, E., Takaku, F. and Yazaki, Y. (1990) Stretching cardiac myocytes stimulates protooncogene expression. *J Biol Chem*, 265, 3595-3598.

Lanctot, P.M., Leclerc, P.C., Escher, E., Leduc, R. and Guillemette, G. (1999) Role of N-glycosylation in the expression and functional properties of human AT1 receptor. *Biochemistry*, 38, 8621-8627.

Lemaire, K., Van de Velde, S., Van Dijck, P. and Thevelein, J.M. (2004) Glucose and sucrose act as agonist and mannose as antagonist ligands of the G protein-coupled receptor Gpr1 in the yeast Saccharomyces cerevisiae. *Mol Cell*, 16, 293-299.

Miura, S., Feng, Y.H., Husain, A. and Karnik, S.S. (1999) Role of aromaticity of agonist switches of angiotensin II in the activation of the AT1 receptor. *J Biol Chem*, 274, 7103-7110.

Miura, S. and Karnik, S.S. (2002) Constitutive activation of angiotensin II type 1 receptor alters the orientation of transmembrane Helix-2. *J Biol Chem*, 277, 24299-24305.

Miura, S., Karnik, S.S. and Saku, K. (2005) Constitutively active homo-oligomeric

angiotensin II type 2 receptor induces cell signaling independent of receptor conformation and ligand stimulation. *J Biol Chem*, 280, 18237-18244.

Miura, S., Zhang, J., Boros, J. and Karnik, S.S. (2003) TM2-TM7 interaction in coupling movement of transmembrane helices to activation of the angiotensin II type-1 receptor. *J Biol Chem*, 278, 3720-3725.

Noda, K., Saad, Y., Kinoshita, A., Boyle, T.P., Graham, R.M., Husain, A. and Karnik, S.S. (1995) Tetrazole and carboxylate groups of angiotensin receptor antagonists bind to the same subsite by different mechanisms. *J Biol Chem*, 270, 2284-2289.

Ohyama, K., Yamano, Y., Sano, T., Nakagomi, Y., Hamakubo, T., Morishima, I. and Inagami, T. (1995) Disulfide bridges in extracellular domains of angiotensin II receptor type IA. *Regul Pept*, 57, 141-147.

Palczewski, K., Kumasaka, T., Hori, T., Behnke, C.A., Motoshima, H., Fox, B.A., Le Trong, I., Teller, D.C., Okada, T., Stenkamp, R.E., Yamamoto, M. and Miyano, M. (2000) Crystal structure of rhodopsin: A G protein-coupled receptor. *Science*, 289, 739-745.

Suchyna, T.M., Tape, S.E., Koeppe, R.E., 2nd, Andersen, O.S., Sachs, F. and Gottlieb, P.A. (2004) Bilayer-dependent inhibition of mechanosensitive channels by neuroactive peptide enantiomers. *Nature*, 430, 235-240.

Takezako, T., Gogonea, C., Saad, Y., Noda, K. and Karnik, S.S. (2004) "Network leaning" as a mechanism of insurmountable antagonism of the angiotensin II type 1 receptor by non-peptide antagonists. *J Biol Chem*, 279, 15248-15257.

Thompson, J.D., Higgins, D.G. and Gibson, T.J. (1994) CLUSTAL W: improving the sensitivity of progressive multiple sequence alignment through sequence weighting, position-specific gap penalties and weight matrix choice. *Nucleic Acids Res*, 22, 4673-4680.

Zou, Y., Akazawa, H., Qin, Y., Sano, M., Takano, H., Minamino, T., Makita, N., Iwanaga, K., Zhu, W., Kudoh, S., Toko, H., Tamura, K., Kihara, M., Nagai, T., Fukamizu, A., Umemura, S., Iiri, T., Fujita, T. and Komuro, I. (2004) Mechanical stress activates angiotensin II type 1 receptor without the involvement of angiotensin II. *Nat Cell Biol*, 6, 499-506.

Supplementary Fig. S1

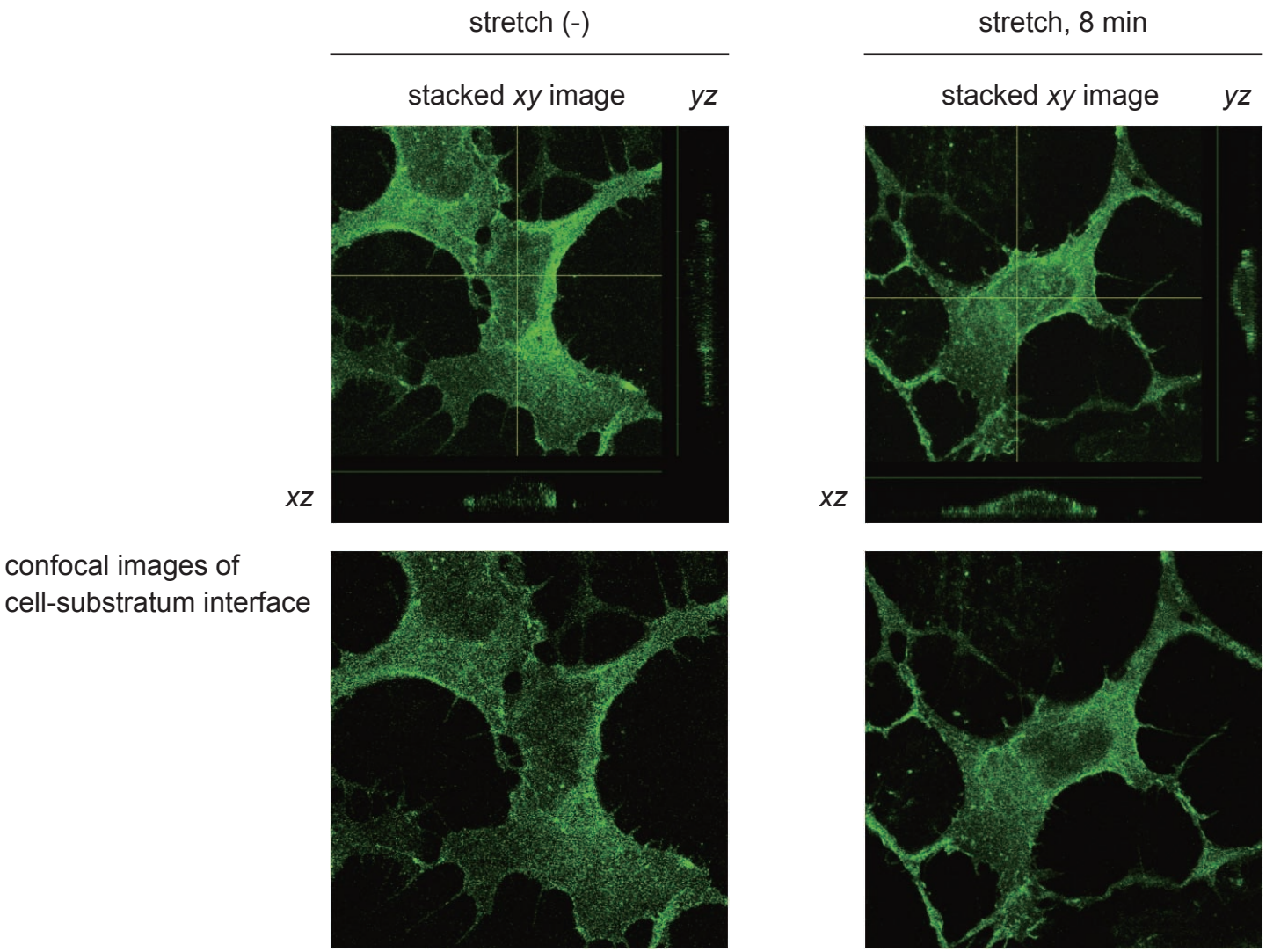

Figure S1. Subcellular distribution of AT_1 receptor in HEK293-AT_1 cells with or without stretch HEK293 cells stably expressing HA-tagged AT_1 receptor were cultured on silicone dishes. The cells were left unstretched or stretched for 8 min, and were stained with anti-HA antibody and visualized with FITC-conjugated secondary antibody through a confocal microscope (upper panels) (Fluo View FV1000; Olympus). Vertical *xz* and *yz* sectional images are shown in each lower and side panel, respectively. The bottom panels are the confocal images showing the cell-substratum interface. AT_1 receptor was predominantly localized in the plasma membrane in static HEK293 cells, and showed uniform distribution at adherent and non-adherent surfaces. At 8 min after stretch, most of AT_1 receptor remained in the plasma membrane. In addition, we confirmed that the *B*max value was unchanged at 8 min after stretch, compared with that before stretch (before stretch; 4.3 ± 0.2 pmol/mg protein, 8 min after stretch; 4.8 ± 0.2 pmol/mg protein).

Supplementary Fig. S2

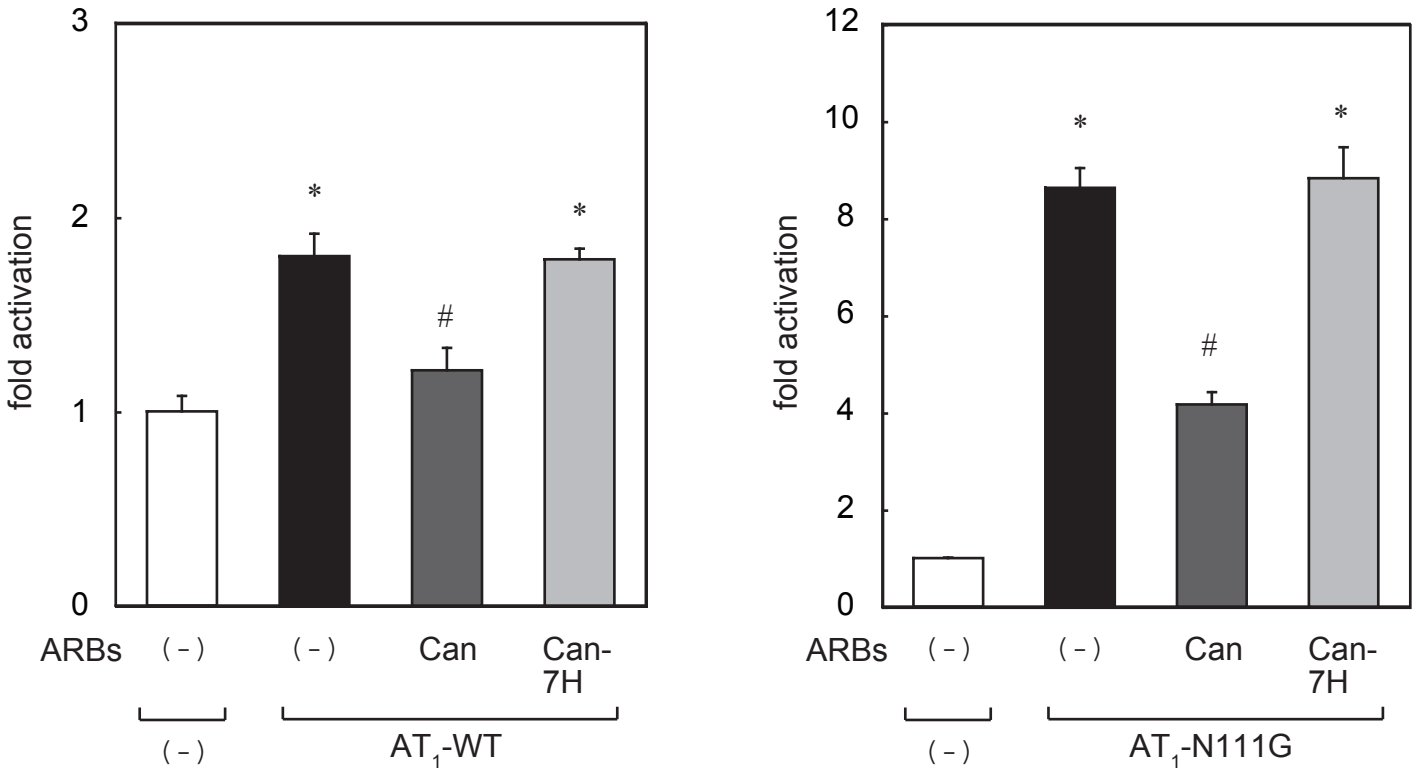

Figure S2. Inhibitory effects of candesartan or candesartann-7H on the basal *c-fos* promoter activities in HEK293 cells expressing AT_1-WT or AT_1-N111G

We previously reported that that AngII increased the promoter activity of *c-fos* gene (Aikawa et al, 2000; Kudoh et al, 1997). The luciferase reporters containing the *c-fos* promoter were co-transfected in HEK293 cells with the expression vector for AT_1-WT or a constitutively active AT_1-N111G mutant receptor. The cells were treated with 10^{-6} M candesartan (Can) or candesartan-7H (Can-7H) 20h before the measurement of luciferase activities. When expressed at a high density, AT_1-WT, as well as AT_1-N111G, showed constitutive luciferase activities in the absence of AngII. Candesartan significantly suppressed the basal *c-fos* promoter activities either by AT_1-WT or AT_1-N111G, but candesartan-7H failed to do so. These results suggest that the carboxyl group of candesartan is required for the potent inverse agonist activity to suppress agonist-independent constitutive activities of AT_1 receptor. *P<0.05 versus mock transfected cells, #P<0.05 versus AT_1-WT transfected cells with no treatment.

Supplementary Fig. S3

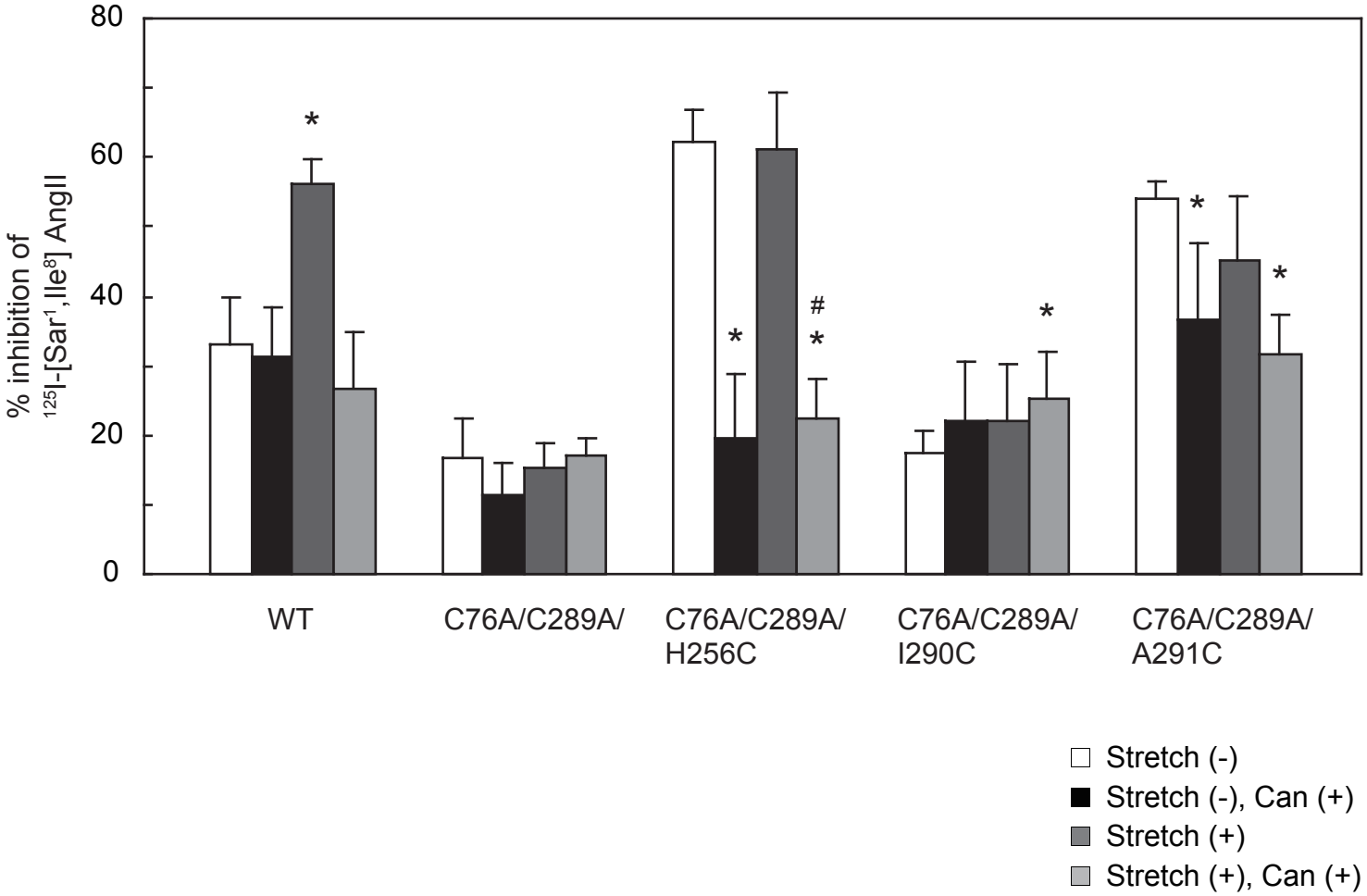

Figure S3. Clockwise rotation of TM VI and VII after stretch in the presence of candesartan
Alteration of cysteine accessibility by mechanical stretch in COS7 cells expressing AT_1 WT, C76A/C289A, C76A/C289A/H256C, C76A/C289A/I290C, or C76A/C289A/A291C receptors. The cells were pretreated with or without 10^{-7} M Can and stretched for 0 or 8 min. The cell membranes were washed and subjected to a SCAM study. After stretch in the presence of candesartan, the % inhibition of ^{125}I-[Sar^1, Ile^8] AngII binding showed a significant increase in C76A/C289A/I290C receptor and a significant decrease in C76A/C289A/A291C receptor. These results suggest that Ile290 becomes accessible to the ligand-binding pocket, while Ala291 goes away from the pocket. Open, closed, dark grey and light grey bars indicate stretch (-), stretch (-) with Can, stretch (+), and stretch (+) with Can, respectively. *P<0.05 versus stretch (-), #P<0.05 versus stretch (+).

Supplementary Fig. S4

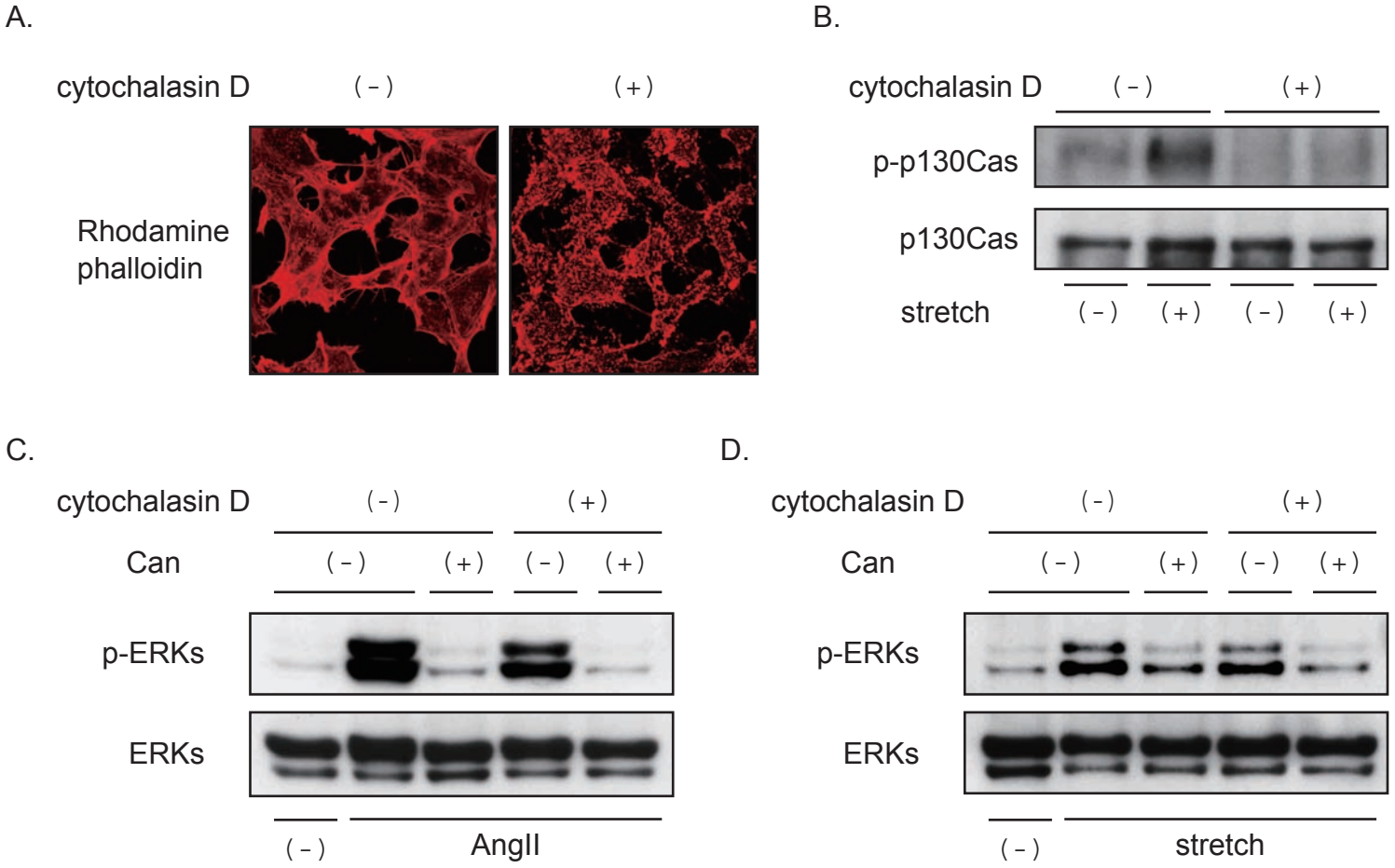

Figure S4. The effect of cytoekeletal breakdown with cytochalasin D on stretch-induced activation of AT_1 receptor

A. Actin staining with rhodamine-conjugated phalloidin demonstrated that treatment with 40 μM cytochalasin D for 10 min inhibited actin polymerization and induced cytoskeletal breakdown in HEK293-AT_1 cells.

B. HEK293-AT_1 cells, pretreated with 40 μM cytochalasin D or vehicle for 10 min, were subjected to mechanical stretch by 20% for 1 min. p130Cas was phosphorylated by mechanical tension transmitted by actin cytoskeletal complex (Sawada and Sheetz, 2002; Sawada et al., 2006). As expected, cytoekeletal breakdown with cytochalasin D abrogated stretch-induced increase in tyrosine phosphorylation of p130Cas on Tyr165 in HEK293-AT_1 cells. p-p130Cas, phosphorylated p130Cas.

C. HEK293-AT_1 cells, pretreated with 40 μM cytochalasin D or vehicle for 10 min, were stimulated with 10^{-7} M AngII for 8 min. Cytoskeletal breakdown did not inhibit AngII-induced phosphorylation of ERKs in HEK293-AT_1 cells, and this activation was significantly inhibited by pretreatment with candesartan (Can). p-ERKs, phosphorylated ERKs.

D. HEK293-AT_1 cells, pretreated with 40 μM cytochalasin D or vehicle for 10 min, were subjected to mechanical stretch by 20% for 8 min. Cytoskeletal breakdown did not inhibit stretch-induced phosphorylation of ERKs in HEK293-AT_1 cells, and this activation was significantly inhibited by pretreatment with candesartan (Can). p-ERKs, phosphorylated ERKs.

Supplementary Fig. S5

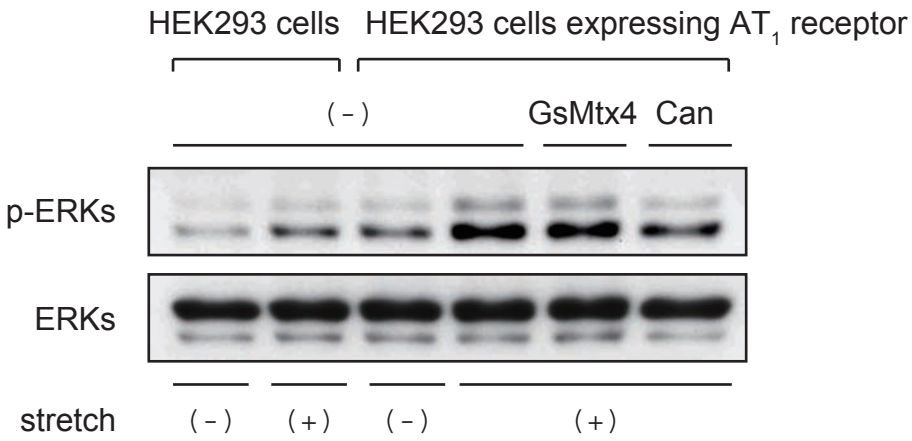

Figure S5. Mechanical stretch activates AT_1 receptor independently of SACs

Although GsMtx-4 has a binding affinity of about 500 nM for SACs in astrocytes (Bode et al., 2001), pretreatment with 2.5 mM GsMtx-4 did not inhibit stretch-induced ERKs activation in HEK293-AT_1 cells.

Supplementary Fig. S6

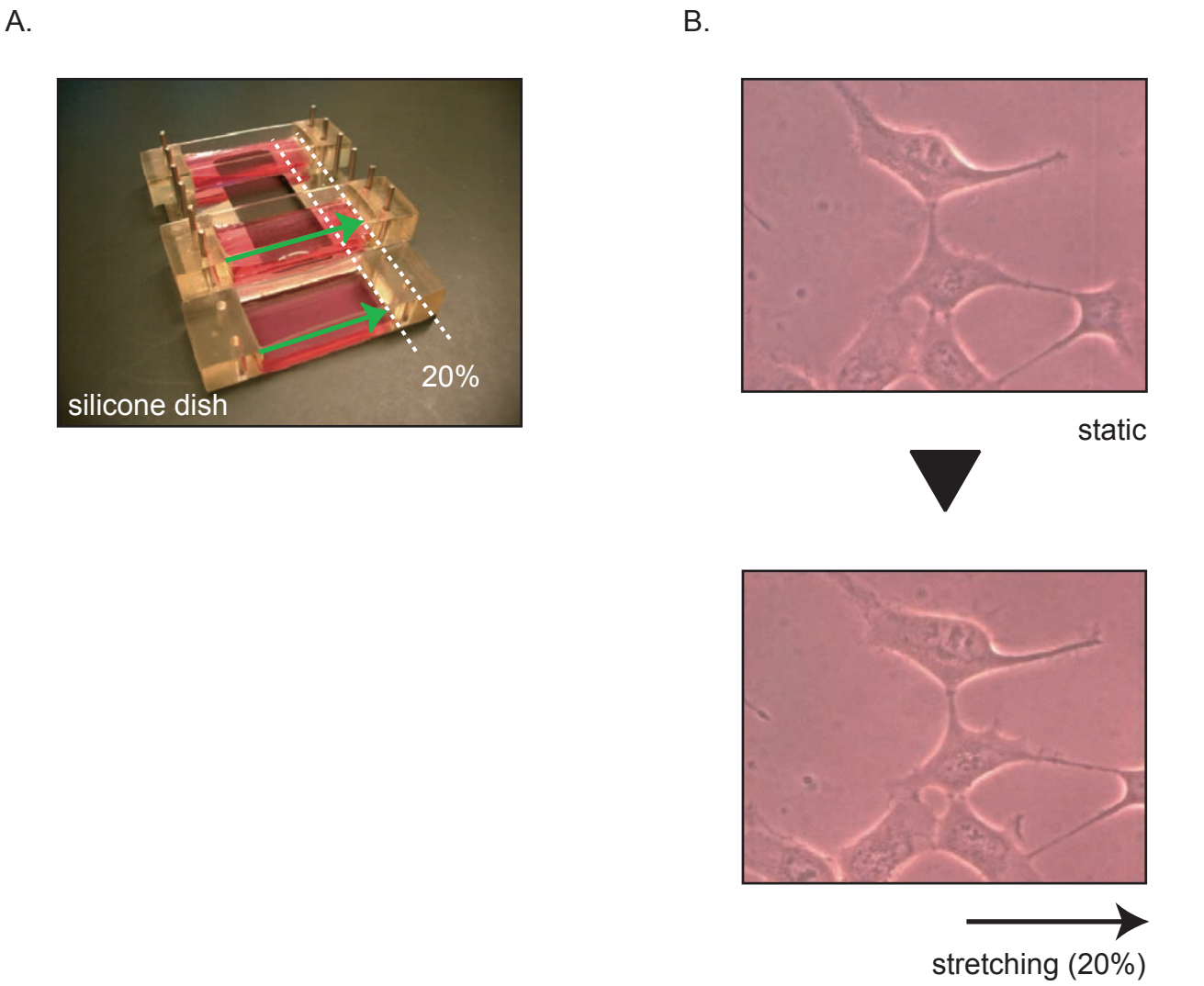

Figure S6. Passive stretch of cells cultured on extensible silicone dishes

A. Cells were plated on collagen-coated silicone rubber dishes, and silicone dishes were passively stretched longitudinally by 20%.

B. HEK293cells before and after stretching were shown as phase-contrast images.

Table S1. Maximal binding capacities (B_{max}) and binding affinities (K_d) of [Sar[1], Ile[8]] AngII to AT1 wild-type (WT) and mutant receptors

Receptor	B_{max} (pmol/mg protein)	K_d (nM)
WT	0.59 ± 0.08	0.7 ± 0.3
C76A	0.52 ± 0.07	0.8 ± 0.2
C121A	0.84 ± 0.14	0.7 ± 0.2
C149A	0.28 ± 0.07	0.5 ± 0.2
C289A	0.31 ± 0.05	1.0 ± 0.1
C296A	0.50 ± 0.03	0.7 ± 0.2
C355A	0.50 ± 0.09	1.2 ± 0.3
C76A/C289A	0.53 ± 0.11	1.8 ± 0.2
C76A/C296A	0.61 ± 0.05	2.6 ± 0.3
C76A/C289A/C296A	0.64 ± 0.08	2.6 ± 0.4
Cys (-)	0.63 ± 0.10	0.7 ± 0.1
C76A/T287C/C289A	0.18 ± 0.06	1.3 ± 0.2
C76A/I288C/C289A	0.21 ± 0.10	2.4 ± 0.3
C76A/C289A/I290C	0.51 ± 0.02	1.0 ± 0.3
C76A/C289A/A291C	0.46 ± 0.12	0.7 ± 0.1
C76A/C289A/Y292C	0.41 ± 0.03	1.1 ± 0.2
C76A/C289A/F293C	0.70 ± 0.03	0.6 ± 0.2
C76A/C289A/N294C	0.56 ± 0.16	0.5 ± 0.2
C76A/C289A/N295C	0.49 ± 0.08	1.3 ± 0.4

Table S2. Maximal binding capacities (B_{max}) and binding affinities (K_d) of [Sar^1, Ile^8] AngII, candesartan and candesartan-7H to AT1 wild-type (WT) and mutant receptors

Receptor	B_{max}	K_d (nM)		
	(pmol/mg protein)	[Sar^1, Ile^8] AngII	candesartan	candesartan-7H
WT	0.52 ± 0.04	0.8 ± 0.3 (1.0)	2.1 ± 0.4 (1.0)	8.4 ± 1.6
H256A	0.38 ± 0.06	0.7 ± 0.3 (0.9)	2.2 ± 0.8 (1.0)	ND
Q257A	0.28 ± 0.16	1.2 ± 0.4 (1.5)	26 ± 6 (12)	ND
T287A	0.43 ± 0.06	1.3 ± 0.2 (1.6)	18 ± 6 (8.6)	ND
Y292A	0.73 ± 0.03	1.5 ± 0.3 (1.9)	5.7 ± 1.5 (2.7)	ND

ND not determined